This article was downloaded by:
On: *26 January 2011*
Access details: *Access Details: Free Access*
Publisher *Taylor & Francis*
Informa Ltd Registered in England and Wales Registered Number: 1072954 Registered office: Mortimer House, 37-41 Mortimer Street, London W1T 3JH, UK

Liquid Crystals
Publication details, including instructions for authors and subscription information:
http://www.informaworld.com/smpp/title~content=t713926090

Novel frequency dependence of dielectric biaxiality of surface stabilized ferroelectric liquid crystals

Nobuyuki Itoh[a]; Mitsuhiro Koden[a]; Shuji Miyoshi[a]; Tadashi Akahane[b]
[a] Central Research Laboratories, SHARP Corporation, Nara, Japan [b] Department of Electrical Engineering, Faculty of Engineering, Nagaoka University of Technology, Niigata, Japan

To cite this Article Itoh, Nobuyuki , Koden, Mitsuhiro , Miyoshi, Shuji and Akahane, Tadashi(1995) 'Novel frequency dependence of dielectric biaxiality of surface stabilized ferroelectric liquid crystals', Liquid Crystals, 18: 1, 109 — 116
To link to this Article: DOI: 10.1080/02678299508036599
URL: http://dx.doi.org/10.1080/02678299508036599

PLEASE SCROLL DOWN FOR ARTICLE

Full terms and conditions of use: http://www.informaworld.com/terms-and-conditions-of-access.pdf

This article may be used for research, teaching and private study purposes. Any substantial or systematic reproduction, re-distribution, re-selling, loan or sub-licensing, systematic supply or distribution in any form to anyone is expressly forbidden.

The publisher does not give any warranty express or implied or make any representation that the contents will be complete or accurate or up to date. The accuracy of any instructions, formulae and drug doses should be independently verified with primary sources. The publisher shall not be liable for any loss, actions, claims, proceedings, demand or costs or damages whatsoever or howsoever caused arising directly or indirectly in connection with or arising out of the use of this material.

LIQUID CRYSTALS, 1995, VOL. 18, NO. 1, 109–116

Novel frequency dependence of dielectric biaxiality of surface stabilized ferroelectric liquid crystals

by NOBUYUKI ITOH*, MITSUHIRO KODEN, SHUJI MIYOSHI
and TADASHI AKAHANE†
Central Research Laboratories, SHARP Corporation, 2613-1 Ichinomoto-cho,
Tenri, Nara 632, Japan
† Department of Electrical Engineering, Faculty of Engineering,
Nagaoka University of Technology, Kamitomioka 1603-1, Nagaoka,
Niigata 940-21, Japan

(*Received 21 April 1994; accepted 25 May 1994*)

The frequency dependence of the dielectric biaxiality of surface stabilized ferroelectric liquid crystals (SSFLCs) was studied. The principal values of the dielectric tensor ε_1, ε_2 and ε_3 were measured by the MOM (molecular orientational model) method. Three dielectric permittivities were measured for each of two samples. These were the permittivity of the homeotropic cell and the permittivity of the planar homogeneous cell with and without the DC bias. Then the dielectric tensor components were calculated based on the molecular orientational models. We present the theory and experimental procedure of the MOM method. Measurements have been performed on Merck FLC compound SCE-8. The following novel dielectric behaviour was observed, as the DC bias voltage was increased the dielectric permittivity of the planar homogeneous cell decreased at the low frequencies (~ 1 kHz) while increased at the high frequencies (10 kHz ~). The sign of the dielectric biaxiality $\partial\varepsilon$ ($= \varepsilon_2 - \varepsilon_1$) inverted around 1 kHz, being negative at low frequencies and positive at high frequencies. The roles of the biaxiality on the dielectric behaviour of SSFLC cells are discussed.

Downloaded At: 10:30 26 January 2011

1. Introduction

The physical parameters of biaxial liquid crystals are very interesting. In particular, the dielectric biaxiality of ferroelectric liquid crystals (FLCs) has a practically very important role. Surface stabilized ferroelectric liquid crystal (SSFLC) [1] devices using the $\tau - V_{\min}$ mode have been reported [2–5]. SSFLC devices utilizing the $\tau - V_{\min}$ mode showed a fast line address time and a high contrast ratio [5]. The dielectric biaxiality is a very important parameter for this type of SSFLC device since in principle the characteristics of the $\tau - V_{\min}$ mode are dominated by the combination of the magnitude of the dielectric biaxiality and the spontaneous polarization [6, 7]. We presented the MOM (molecular orientational model) method to measure the dielectric permittivities of FLC from SSFLC cell directly [8], not from the helical structure [9] or the achiral host material [10, 11]. The validity of the MOM method was confirmed. The obtained principal dielectric permittivities were accurate regardless of differences of the measured dielectric permittivities of the sample cells showing different molecular orientational states. The theory and experimental procedure of the MOM method are explained in § 2. In this study, we measured the frequency dependence of the dielectric permittivities of SSFLC. A novel dielectric behaviour under the DC biasing field and an inversion of the sign of the dielectric biaxiality at the different frequencies were observed for SSFLC cells. The importance of the dielectric biaxiality on the dielectric behaviour of SSFLC cells will be discussed.

2. Theory of MOM dielectric permittivity measurement

The theory of the dielectric permittivity measurement by the MOM method was shown in our previous paper in detail [8]. The principal values of the dielectric permittiv-

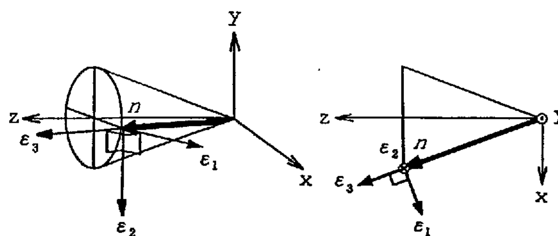

Figure 1. The definition of the principal dielectric permittivities of the FLC.

* Author for correspondence.

0267–8292/95 $10·00 © 1995 Taylor & Francis Ltd.

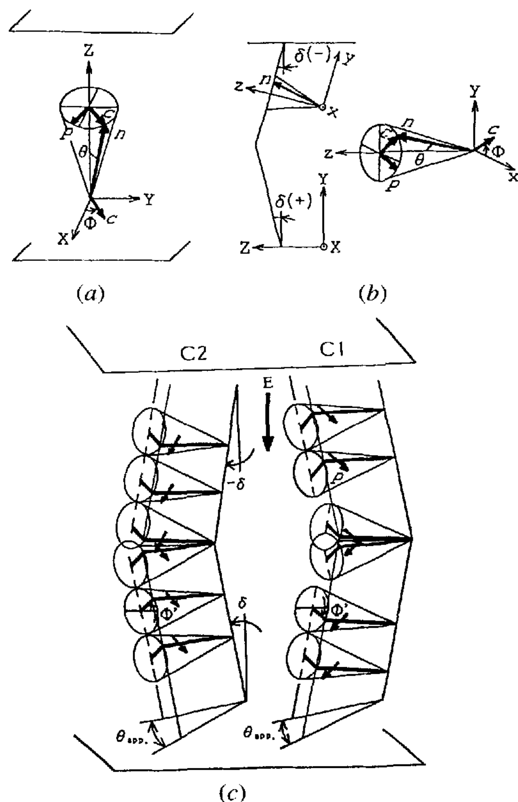

Figure 2. The geometries of the dielectric permittivity measurement. (*a*) Homeotropic cell. (*b*) Planar homogeneous cell. (*c*) Homogeneous cell under DC bias.

ity tensor of FLCs are defined as in previous reports [9–11], and as shown in figure 1. Three principal dielectric permittivities are denoted as ε_1, ε_2 and ε_3. ε_1 denotes the permittivity in the tilt plane made by the symmetry axis of the smectic cone z and the director n, perpendicular to the long molecular axis. ε_2 denotes the permittivity in the direction perpendicular to the long molecular axis and to the tilt plane, in the direction of the spontaneous polarization. ε_3 denotes the permittivity in the direction of the long molecular axis. Two dielectric anisotropies are defined as $\Delta\varepsilon = \varepsilon_3 - \varepsilon_1$ and $\partial\varepsilon = \varepsilon_2 - \varepsilon_1$, where $\partial\varepsilon$ is the dielectric biaxiality. The dielectric permittivity tensor in the local frame is defined as

$$\bar{\varepsilon}(1,2,3) = \begin{pmatrix} \varepsilon_1 & 0 & 0 \\ 0 & \varepsilon_2 & 0 \\ 0 & 0 & \varepsilon_3 \end{pmatrix}. \tag{1}$$

The MOM method requires two differently aligned sample cells and uses three geometric systems which are illustrated in figure 2. Here θ, δ, ϕ and θ_{app} are the tilt angle, the layer tilt angle, the azimuthal angle and the apparent tilt angle, respectively. The first system is the homeotropic geometry for which the smectic layers are parallel to the electrode planes (see figure 2 (*a*)). The measured dielectric permittivity of the homeotropic cell is

$$\begin{aligned} \varepsilon_{\mathrm{h}} &= \varepsilon_1 \sin^2\theta + \varepsilon_3 \cos^2\theta \\ &= \varepsilon_1 + \Delta\varepsilon \cos^2\theta. \end{aligned} \tag{2}$$

The second system is a planar homogeneous geometry with the chevron layer structure (see figure 2 (*b*)). In this geometry the azimuthal angle of the director varies across the cell and strongly depends on the molecular orientational states, as shown in figure 3 [12–14]. Figure 3 shows the orientational models of SSFLC cells with parallel rubbing which are described by the combination of two classifications, the uniform (U) and twisted (T) states [15, 16], and the C1 and C2 states [17]. The former classification is based on the optical viewing behaviour when the sample cell is placed between crossed polarizers without any field. The uniform state shows extinction positions, but the twisted state shows only colouration positions without any extinction. The latter classification is based on the relationship between the direction of the chevron layer structure and the direction of the surface pretilt. The boundary surfaces in the C2 state do not have wide regions over which the molecules can exist stably. The c-directors at the surfaces are almost perpendicular to the substrates in the C2 model if the surface pretilt angle is larger than the difference between the tilt angle (half of the cone angle) and the layer tilt angle. This type of C2 state is defined as a special case of the C2U state, called the high pretilt C2U state. The distribution of the director across the cell is very different for each of the molecular orientational states. The dielectric permittivities should be measured considering the distribution of the director. The measured dielectric permittivity of a planar homogeneous

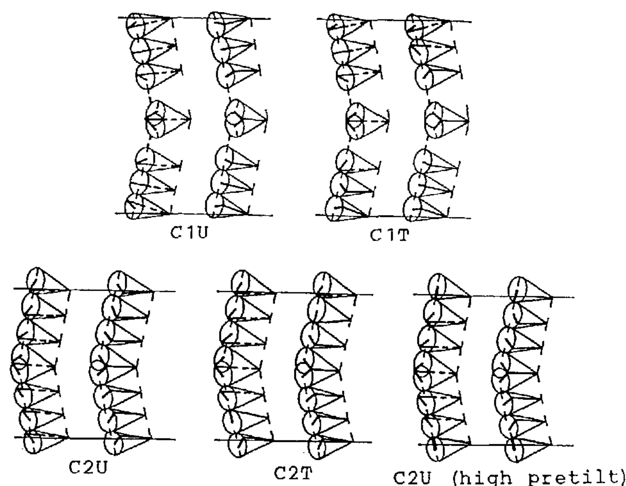

Figure 3. The molecular orientational models of SSFLCs with a chevron layer structure.

Downloaded At: 10:30 26 January 2011

cell is expressed as

$$\frac{1}{\varepsilon_p}=\frac{1}{d}\int_0^{d/2}\frac{1}{\varepsilon_{YY}}dY+\int_{d/2}^{d}\frac{1}{\varepsilon_{YY}}dY$$
$$=\frac{1}{2(\phi_{in}-\phi_0)}\int_{\phi_0}^{\phi_{in}}\frac{1}{\varepsilon_{YY}}d\phi+\frac{1}{2(\phi_d-\phi_{in})}\int_{\phi_{in}}^{\phi_d}\frac{1}{\varepsilon_{YY}}d\phi, \tag{3}$$

where ε_{YY} is the component of the permittivity tensor in the direction of the electric field and is expressed as

$$\varepsilon_{YY}=\varepsilon_1+\Delta\varepsilon[\sin\theta\cos\delta\sin\phi(Y)-\cos\theta\sin\delta]^2$$
$$+\partial\varepsilon\cos^2\delta\cos^2\phi(Y). \tag{4}$$

The azimuthal angle ϕ is a function of the cell normal Y, and d is the cell thickness. ϕ_0, ϕ_d, and ϕ_{in} are the azimuthal angles at the bottom and top surfaces, and at the chevron interface, respectively. The azimuthal angle at the surfaces are expressed as

$$\left.\begin{aligned}\phi_0&=\sin^{-1}\left(\frac{\tan\delta}{\tan\theta}+\frac{\sin\theta_p}{\sin\theta\cos\delta}\right),\\ \phi_d&=\sin^{-1}\left(\frac{\tan(-\delta)}{\tan\theta}+\frac{\sin\theta_p}{\sin\theta\cos(-\delta)}\right),\end{aligned}\right\} \tag{5}$$

where θ_p is the surface pretilt angle. The azimuthal angle at the chevron interface is expressed as

$$\phi_{in}=\sin^{-1}(\tan\delta/\tan\theta). \tag{6}$$

It should be noted that the sign of δ is opposite for the C1 and C2 states, and the sign of θ_p is also opposite at the bottom and top surfaces. It is assumed that ϕ_0 is $\pi/2$ and ϕ_d is $-\pi/2$ in the high pretilt C2U model. The azimuthal angle ϕ is assumed to change with the cell thickness direction Y at a constant rate in each part of the chevron layer structure, and equations (7) and (8) are applied to the transformation in equation (3)

$$\left.\begin{aligned}\frac{1}{d}\int_0^{d/2}\frac{1}{\varepsilon_{YY}}dY&=\frac{1}{d}\int_{\phi_0}^{\phi_{in}}\frac{1}{\varepsilon_{YY}}\frac{dY}{d\phi}d\phi,\\ \frac{1}{d}\int_{d/2}^{d}\frac{1}{\varepsilon_{YY}}dY&=\frac{1}{d}\int_{\phi_{in}}^{\phi_d}\frac{1}{\varepsilon_{YY}}\frac{dY}{d\phi}d\phi.\end{aligned}\right\} \tag{7}$$

$$\left.\begin{aligned}\frac{d\phi}{dY}&=\frac{\phi_{in}-\phi_0}{(d/2)}=\text{const.}\quad(0\leqq Y\leqq d/2),\\ \frac{d\phi}{dY}&=\frac{\phi_d-\phi_{in}}{(d/2)}=\text{const.}\quad(d/2<Y\leqq d).\end{aligned}\right\} \tag{8}$$

The optical simulations using the molecular orientational models in figure 3 showed good agreement with optical measurement results using equations (7) and (8) [12–14].

The last system is the planar homogeneous chevron geometry with a constant azimuthal angle ϕ' under the DC bias (see figure 2 (*c*)). The measured dielectric permittivity of a planar homogeneous cell under the DC bias is given by

$$\varepsilon_p'=\varepsilon_1+\Delta\varepsilon(\sin\theta\sin\phi'\cos\delta-\cos\theta\sin\delta)^2$$
$$+\partial\varepsilon\cos^2\phi'\cos^2\delta. \tag{9}$$

The measurement must be performed under the condition of no smectic layer deformation. We have reported that the dielectric permittivity after an electric field treatment began to change when the texture changed from the initial state to the rooftop texture and increased with increasing density of rooftop lines, beginning to saturate when the striped texture appeared. The fact that deformation of the smectic layer structure caused by an electric field treatment changed the dielectric permittivity of the SSFLC was confirmed [18]. This change in dielectric behaviour was consistent with the deformation process of the smectic layer structure. The appropriate bias voltage can be determined by checking the dielectric permittivity after the biasing and by texture observation. The constant azimuthal angle ϕ' when the appropriate bias voltage is applied, is determined from the voltage dependence of the apparent tilt angle θ_{app}, together with the simulation of the azimuthal angle dependence of the apparent tilt angle. Figure 2 (*c*) shows the relationship between ϕ' and θ_{app}. The apparent tilt angle θ_{app} is expressed as

$$\theta_{app}=\tan^{-1}\left(\frac{\sin\theta\cos\phi'}{\sin\theta\sin\phi'\sin\delta+\cos\theta\cos\delta}\right). \tag{10}$$

The three principal dielectric permittivities, ε_1, ε_2 and ε_3 are calculated from three experimental measured values of the equations (2), (3) and (9) by a coordinate transformation using figures 2 and 3. In particular, defect-free homogeneous molecular orientational states are required in order to solve equations (3)–(8) of the planar homogeneous cell.

3. Experimental

An FLC material SCE-8 (E. Merck Ltd.) was used to measure the dielectric permittivities in this study. The layer tilt angle measured by X-ray diffraction was 19·5°, the tilt angle measured by a polarized microscope and corrected by the layer tilt angle was 21°, both values at 25°C [14]. The homeotropic cell was made using the polyimide aligning film JALS-204 (Japan Synthetic Rubber Co., Ltd.). Two kinds of planar homogeneous cells rubbed in parallel directions were made using the polyimide aligning films PSI-A-2001 (Chisso Co., Ltd.) and PI-A, respectively. These polyimide aligning films were formed on glass plates with an ITO electrode by spincoating and were then baked. The cell thickness was controlled to around 6 μm for the homeotropic cell and was around 1·5 μm for the planar homogeneous cells by using the silica ball spacers. A SiO_2 insulating layer was used in

Downloaded At: 10:30 26 January 2011

thin planar homogeneous cells between the electrodes and the aligning films to avoid electric contact between the substrates. Antiparallel thick cells (about 50 μm) filled with the nematic liquid crystal E-8 (E. Merck Ltd.) were fabricated to measure the pretilt angles of PI-A and PSI-A-2001. The pretilt angles θ_p were determined to be 5° for PI-A and 15° for PSI-A-2001 by capacitance–magnetic field curves (C–H curves) [19]. According to Kanbe *et al.* [17], it is difficult for the C2 state to appear if the surface pretilt angle is large or the tilt angle is small. The cells were positioned under the crossed nicols of an Olympus polarizing microscope and the texture was observed. The memory angle θ_m was defined as the half-angle between two extinction positions when no field was applied. The apparent tilt angle θ_{app} was defined as the half-angle between two extinction positions when the electric field was applied. The dielectric permittivities were determined from capacitance measurements using a Hewlett Packard precision LCR meter (HP4284A).

4. Results

The cell using PI-A (cell *A*) showed a stable defect-free homogeneous C2U state, and the cell using PSI-A-2001 (cell *B*) showed a defect-free homogeneous C1U state by slow cooling down (-1°C min^{-1}) from the isotropic phase under an applied electric field ($\pm 3{\cdot}3$ V μm^{-1}) [8]. In accordance with previous papers [12–14], the molecular orientation of the defect-free homogeneous state was distinguished by the memory angle. The relationship between the surface pretilt angle and the memory angle has been reported [14]. The memory angle θ_m of cell *A* was 6·5° and that of cell *B* was 13°. The molecular orientational model for cell A is therefore the high pretilt C2U state because the surface pretilt angle is larger than the difference between the tilt angle and the layer tilt angle. Figure 4 shows the behaviour of the dielectric permittivity of the homeotropic cell. Figure 4 (*a*) shows the temperature dependences at the different frequencies and figure 4 (*b*) shows the frequency dependence at 25°C. The dielectric permittivity of the homeotropic cell showed a frequency dispersion in the S_C^* phase and a different temperature dependence at the different frequencies. The dielectric permittivities of the planar homogeneous cells were measured with a 100 mV$_{rms}$ capacitance probe voltage at 25°C. The spontaneous polarization is required to be rotated by the bias field not the capacitance probe voltage. In the dielectric permittivity measurements of the planar homogeneous cells, + DC bias and − DC bias were applied alternately for 5 s each, and repeated 5 times. The dielectric permittivities during biasing and after biasing, when the bias field is turned off, were measured as the voltage was increased. Figures 5 and 6 show the voltage dependence of the dielectric permittivities during biasing and after biasing, respectively. Both the dielectric

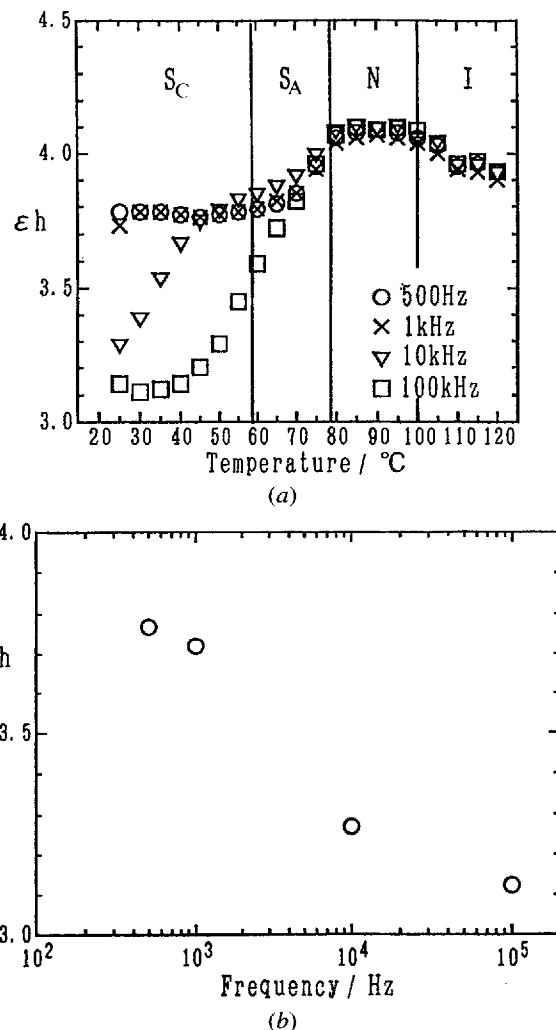

Figure 4. The behaviour of the measured dielectric permittivity of the homeotropic cell. (*a*) The temperature dependences at different frequencies. (*b*) The frequency dependence at 25°C.

permittivities during biasing and after biasing showed a different bias voltage dependence at different frequencies. The dielectric permittivity during biasing shown in figure 5 increased at 10 kHz and 100 kHz with increasing bias voltage; on the other hand it decreased at 500 Hz. At 1 kHz, cell *A* did not show a large change in permittivity and cell *B* showed only slight decrease. Though the magnitudes of the dielectric permittivity of the two cells were different, the bias voltage dependences of the dielectric permittivity showed similar properties. The dielectric permittivities after biasing, shown in figure 6, changed showing a threshold with increasing voltage. The dielectric permittivity after biasing also increased at 10 kHz and 100 kHz, decreased at 500 Hz and did not show a large change at 1 kHz, all for increasing bias voltage. The dielectric permittivity after biasing began to change above 10 V.

Downloaded At: 10:30 26 January 2011

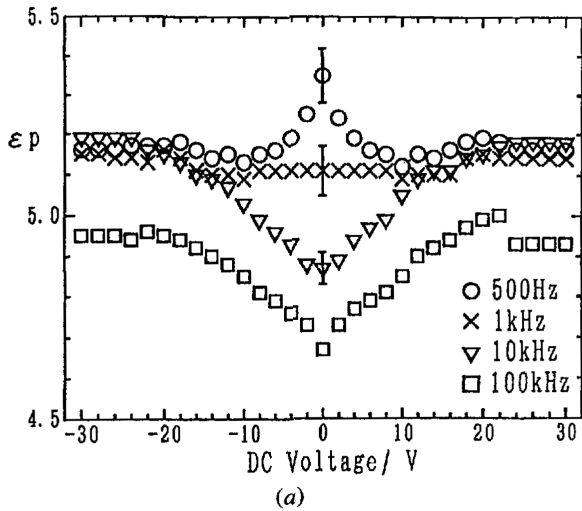

(*a*)

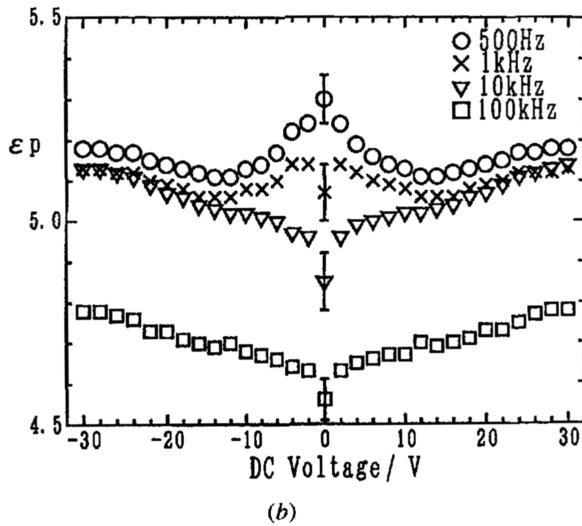

(*b*)

Figure 5. The voltage dependences of the measured dielectric permittivities of the planar homogeneous cells during biasing of (*a*) cell *A* and (*b*) cell *B*.

Above this voltage, the texture changed from the initial state to the rooftop texture. The permittivity increased with the increasing density of rooftop lines, and began to saturate when the striped texture perpendicular to the smectic layers appeared. Therefore, as we mentioned in § 2, it was found that the smectic layer structure did not change below 8 V bias application, according to figure 6. The dielectric permittivity did not depend on the application time of the bias for low bias voltages below 8 V, which was before the texture change. However the dielectric permittivity was dependent on the application time under high bias voltages over 10 V because the texture change and the smectic layer deformation depend on the voltage, frequency and duration of the applied electric field [20, 21]. For the measurements at over 10 V biasing, the final permittivity values during biasing are shown in figure 5. Figure 7 shows the voltage dependence of the apparent tilt angles. Due to the texture changed after 10 V measurement, the apparent tilt angles were measured for this changed texture. Figure 8 shows the simulated azimuthal angle dependence of the apparent tilt angles calculated by equation (10). The constant azimuthal angle ϕ' was determined from figures 7 and 8. Figure 8 was calculated for the half of the chevron layer structure in figure 2 (*c*) between the bottom surface and the chevron interface, and for the range of ϕ' from $-\pi/2$(rad) [$-90°$] to $\pi/2$(rad) [$90°$]. It was assumed that ϕ' lay between its initial value when no field was applied in figure 3 and 0 (rad) as shown in figure 2 (*c*). The apparent tilt angle θ_{app} of cell *A* was 17·0° and that of cell *B* was 21·0°, both at 8 V (see figure 7). The azimuthal angles ϕ of the C2 state when the apparent tilt angle θ_{app} is 17·0°, are $-47·5°$ and 35·5°. Those of the C1 state when θ_{app} is 21·0°, are $-13·5°$ and 28° (see figure 2 (*c*)). The constant azimuthal angle ϕ'

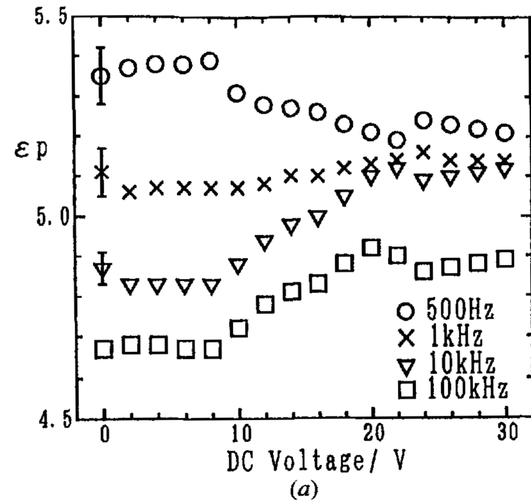

(*a*)

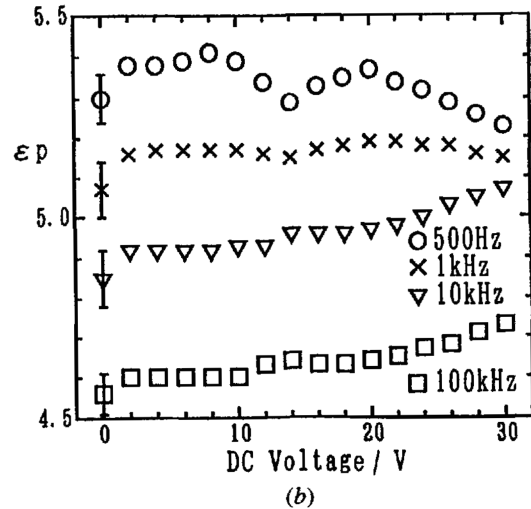

(*b*)

Figure 6. The voltage dependences of the measured dielectric permittivities of the planar homogeneous cells after the biasing field is turned off of (*a*) cell *A and* (*b*) cell *B*.

Downloaded At: 10:30 26 January 2011

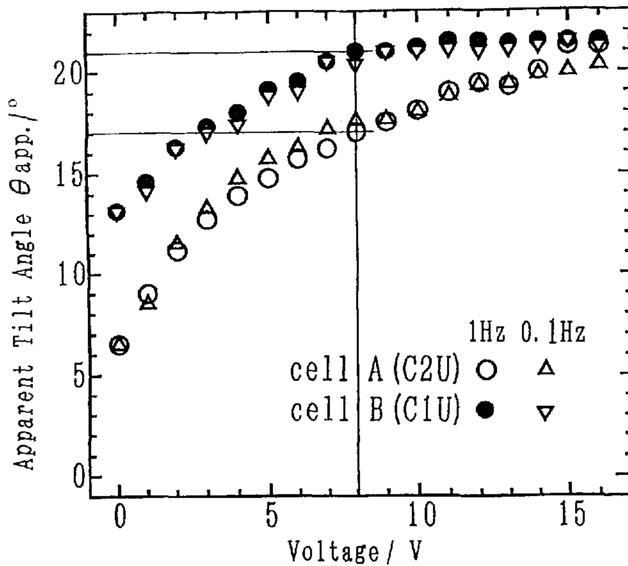

Figure 7. The voltage dependences of the apparent tilt angles of the planar homogeneous cells.

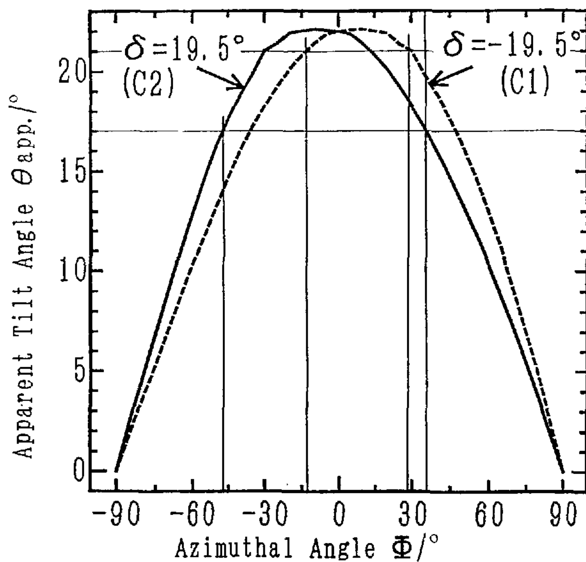

Figure 8. The simulated azimuthal angle dependences of the apparent tilt angles. See text for an explanation of the figure.

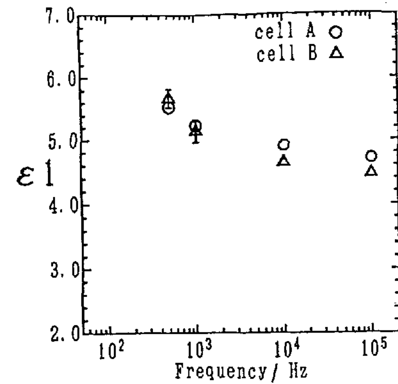

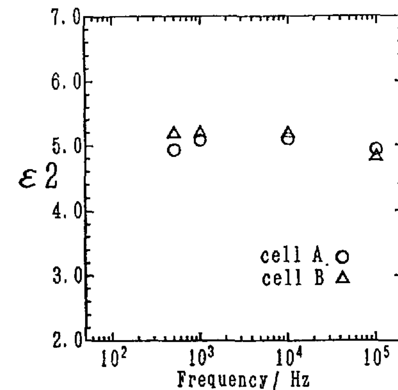

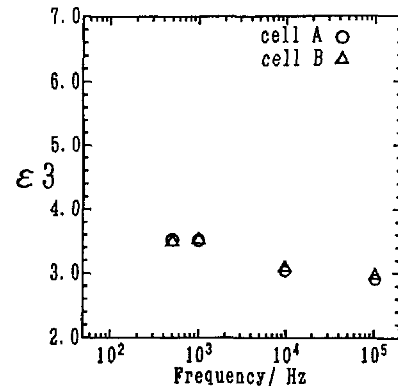

Figure 9. The frequency dependence of principal dielectric permittivities.

in the lower half of the chevron layer structure lies between 0(rad) and $\pi/2$(rad) for the C2 state, and between $-\pi/2$(rad) and 0(rad) for the C1 state, respectively. The constant azimuthal angle ϕ' was determined to be 35·5° for cell *A* and − 13·5° for cell *B* at 8 V bias. The whole chevron layer structure was treated as symmetric about the chevron interface. The three principal dielectric permittivities, calculated using the above procedure, are shown in figure 9. These principal dielectric permittivities ε_1, ε_2 and ε_3 are almost equal for the two cells regardless of the different measured apparent permittivities.

5. Discussion

Before considering the dielectric biaxiality study, we should discuss the influence of the SiO_2 insulating layer on the MOM dielectric permittivity measurement because the insulating layer works as the barrier of the electric field, reducing the voltage across the SSFLC layer. In order to evaluate this effect, an SSFLC cell using PSI-A-2001 without an SiO_2 layer was made. Unfortunately, this cell did not show a homogeneous molecular orientation, giving C1T and C2U states in the electrode area. This meant that we could not measure the accurate dielectric permittivi-

Downloaded At: 10:30 26 January 2011

ties. However the effect of the insulating layer could still be studied. The voltage dependences of the dielectric permittivities at 10 kHz during biasing for cells both with and without an SiO_2 layer are shown in figure 10. The measured dielectric permittivity of the cell without an SiO_2 increased more sharply with voltage than that of the cell with an SiO_2 (cell *B*). This indicates that the bias voltage was certainly reduced by the insulating layer. And so the voltage of the applied electric field used in the apparent tilt angle measurements is also reduced by the barrier effect of the insulating layer. The voltage reduction caused by the insulating layer on the MOM dielectric permittivity measurement is negligible if the bias voltage for the dielectric permittivity measurement in figure 5 and the applied electric field of the apparent tilt angle measurement in figure 7 are equal. We reported the principal dielectric permittivities calculated using the apparent tilt angles measured by a 1 Hz square wave [8]. The apparent tilt angles measured by a 0·1 Hz square wave which is similar to the bias condition are shown in figure 7 (the electric field which is + DC and − DC for 5 s each is equal to a square wave which has a half cycle of 5 s: the frequency of this wave is 0·1 Hz). There were no differences between the apparent tilt angles measured by 1 Hz and 0·1 Hz. In conclusion on the matter of the cell structure, the dielectric permittivities measured by the MOM method are not effected by the barrier layer.

Two dielectric anisotropies, $\Delta\varepsilon$ and the dielectric biaxiality $\partial\varepsilon$, are shown in figure 11. Both $\Delta\varepsilon$ and $\partial\varepsilon$ showed a similar slight frequency dependence. In particular $\partial\varepsilon$ showed an inversion around 1 kHz. It was negative at 500 Hz, almost zero at 1 kHz, and then positive at 10 kHz and 100 kHz. The different frequency dependences of both the apparent dielectric permittivities during biasing in

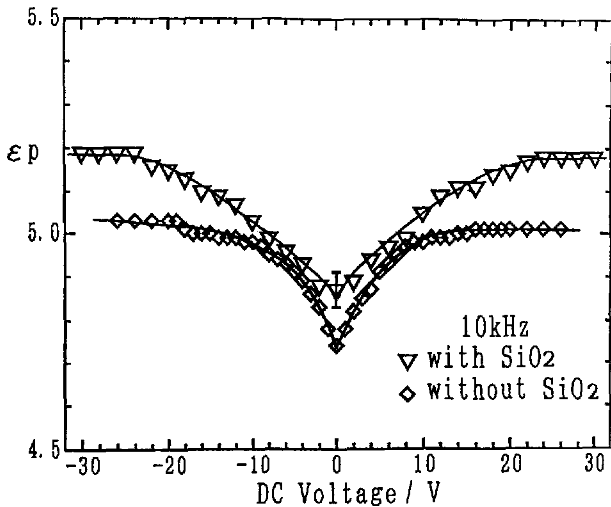

Figure 10. The voltage dependences of the dielectric permittivities at 10 kHz during biasing both with and without an SiO_2 barrire layer.

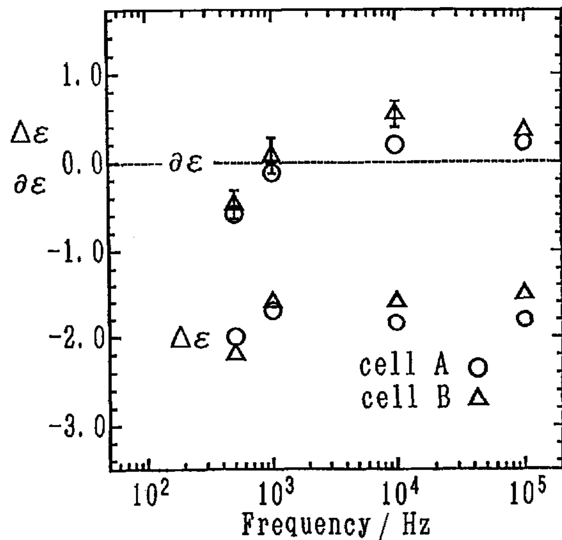

Figure 11. The frequency dependence of the two dielectric anisotropies, $\Delta\varepsilon$ and the dielectric biaxiality $\partial\varepsilon$.

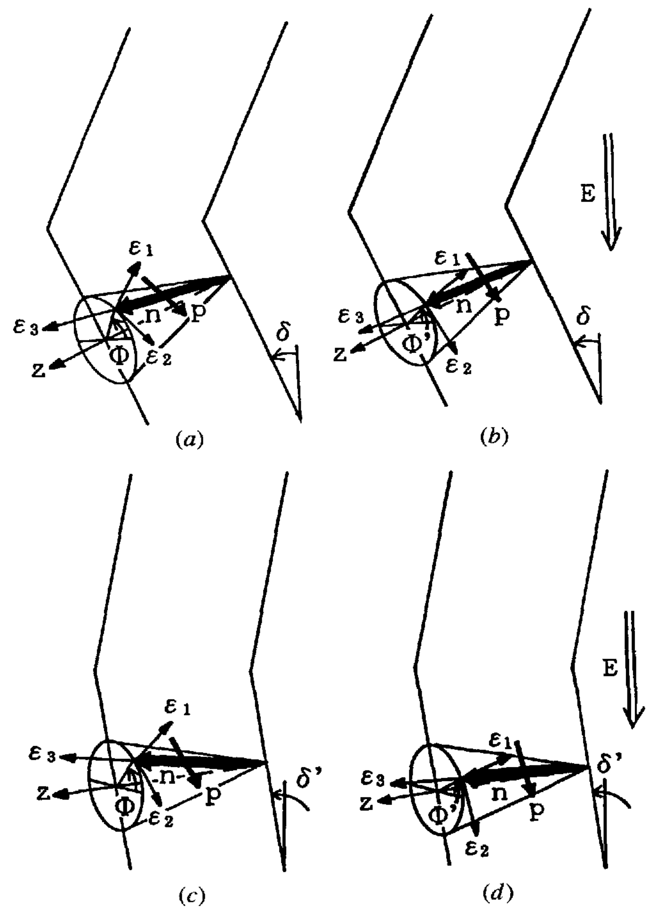

Figure 12. The movement of the FLC molecule on the smectic cone during biasing and after biasing.

Downloaded At: 10:30 26 January 2011

figure 5 and after biasing in figure 6 are explained by this novel frequency dependence of the dielectric biaxiality. The movement of the FLC molecule on the smectic cone is illustrated in figure 12. The component of ε_2 in the dielectric permittivity of the SSFLC cell is increased by the bias field due to the rotation of the spontaneous polarization **p** towards to the direction of the field (see figure 12 (*a*) and (*b*)). The smectic layer deformation from the chevron to the quasi-bookshelf structure also increases the component of ε_2 (see figure 12 (*a*) and (*c*)). Figure 12 (*d*) shows the SSFLC structure during biasing after the smectic layer deformation. As reported previously [18, 20, 21], the smectic layer deformation progresses with increasing electric field treatment voltage. In this study it is the bias voltage which can cause smectic layer deformation. With increasing the bias voltage, both the dielectric permittivities during biasing and after biasing increase if $\partial\varepsilon$ is positive, decrease if $\partial\varepsilon$ is negative and do not change if $\partial\varepsilon$ is zero. Therefore it is found that the movement of the FLC molecule on the smectic cone is strongly dominated by the dielectric biaxiality $\partial\varepsilon$. Let us return to figure 9 in order to discuss this novel behaviour of the dielectric biaxiality with frequency. The dielectric permittivity ε_1 shows an obvious frequency dispersion, while ε_2 and ε_3 only slightly depend on the frequency. The theoretical explanation of these different frequency dependences of three dielectric permittivities is an interesting topic for a later paper.

The authors thank Professor E. P. Raynes and Dr P. A. Gass of Sharp Laboratories of Europe Ltd. for helpful discussions and suggestions.

References

[1] CLARK, N.A., and LAGERWALL, S. T., 1980, *Appl. Phys. Lett.*, **36**, 899.

[2] ORIHARA, H., NAKAMURA, K., ISHIBASHI, Y., YAMADA, Y., YAMAMOTO, N., and YAMAWAKI, M., 1986, *Jap. J. appl. Phys.*, **25**, L839.

[3] SURGUY, P. W. H., AYLIFFE, P. J., BIRCH, M. J., BONE, M. F., COULSON, I., CROSSLAND, W. A., HUGHES, J. R., ROSS, P. W., SAUNDERS, F. C., and TOWLER, M. J., 1991, *Ferroelectrics*, **122**, 63.

[4] HUGHES, J. R., and RAYNES, E. P., 1993, *Liq. Crystals*, **13**, 597.

[5] KODEN, M., KATSUSE, H., ITOH, N., KANEKO, T., TAMAI, K., TAKEDA, H., SHIOMI, M., NUMAO, T., KIDO, M., MATSUKI, M., MIYOSHI, S., and WADA, T., 1993, *Ferroelectrics*, **149**, 183.

[6] JONES, J. C., TOWLER, M. J., and RAYNES, E. P., 1991, *Ferroelectrics*, **121**, 91.

[7] TOWLER, M. J., JONES, J. C., and RAYNES, E. P., 1992, *Liq. Crystals*, **11**, 365.

[8] ITOH, N., KODEN, M., MIYOSHI, S., WADA, T., and AKAHANE, T., 1993, *Ferroelectrics*, **147**, 327.

[9] GOUDA, F., KUCZYNSKI, W., LAGERWALL, S. T., MATUSZCZYK, M., MATUSZCZYK, T., and SKARP, K., 1992, *Phys. Rev.* A, **46**, 951.

[10] JONES, J. C., RAYNES, E. P., TOWLER, M. J., and SAMBLES, J. R., 1991, *Molec. Crystals liq. Crystals*, **199**, 277.

[11] JONES, J. C., and RAYNES, E. P., 1992, *Liq. Crystals*, **11**, 199.

[12] ITOH, N., KODEN, M., MIYOSHI, S., and WADA, T., 1992, *Jap. J. appl. Phys.*, **31**, 852.

[13] ITOH, N., KIDO,, M., TAGAWA, A., KODEN, M., MIYOSHI, S., and WADA, T., 1992, *Jap. J. appl. Phys.*, **31**, L1089.

[14] ITOH, N., KODEN, M., MIYOSHI, S., and WADA, T., 1993, *Liq. Crystals*, **15**, 669.

[15] HANDSCHY, M. A., CLARK, N. A., and LAGERWALL, S. T., 1983, *Phys. Rev. Lett.*, **51**, 471.

[16] OUCHI, Y., TAKEZOE, H., and FUKUDA, A., 1987, *Jap. J. appl. Phys.*, **26**, 1.

[17] KANBE, J., INOUE, H., MIZUTOME, A., HANYUU, Y., KATAGIRI, K., and YOSHIHARA, S., 1991, *Ferroelectrics*, **114**, 3.

[18] ITOH, N., KODEN, M., MIYOSHI, S., WADA, T., and AKAHANE, T., 1994, *Jap. J. appl. Phys.*, **33**, L241.

[19] SUZUKI, K., TORIYAMA, K., and FUKUHARA, A., 1978, *Appl. Phys. Lett.*, **33**, 561.

[20] SATO, Y., TANAKA, T., KOBAYASHI, H., AOKI, K., WATANABE, H., TAKESHITA, H., OUCHI, Y., TAKEZOE, H., and FUKUDA, A., 1989, *Jap. J. appl. Phys.*, **28**, L483.

[21] ISOGAI, M., OH-E, M., KITAMURA, T., and MUKOH, A., 1991, *Molec. Crystals liq. Crystals*, **207**, 87.

Downloaded At: 10:30 26 January 2011